Chapter 6

Characterization of chitosan and Modified chitosan Nanoparticles

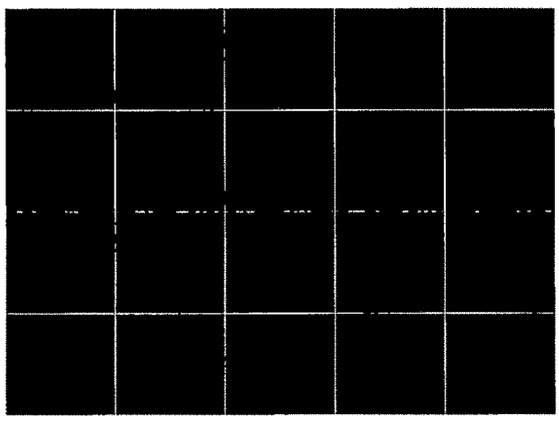

6.1. Introduction

Colloidal systems like nanoparticles differ from macroscopic objects because of sub-micron properties such as high surface area, energy and movement of the particles by diffusion (Brownian motion). The different behaviour of nanoparticles leads, to some extent, to the use of a different pattern of characterization methods. Extensive characterization of a nanoparticles system is essential for understanding and prediction of the performance of the system in the body. As the field of pharmaceutical nanoconstructs is evolving constantly; the need for more thorough characterization and comprehensive understanding of the systems increases. Size, morphology and physical state of the encapsulated drug as well as molecular weight and crystallinity of the polymer influence drug release and degradation of the nanoparticles. Meanwhile, size, surface charge and hydrophobicity/hydrophilicity are parameters that affect the body distribution and interactions with the biological environment. Stability of nanoparticles is also a general issue governing the above mentioned properties.

Various techniques for characterization of nanoparticles include:

- Photon correlation spectroscopy (PCS), a technique based on dynamic (laser) light scattering, is widely used in size determinations of nanoparticles.
- The surface charge of the particle was determined by Zeta(ζ) Potential measurement
- The determination of drug entrapment efficiency by techniques of spectrophotometry and chromatography gives the amount of drug present in the nanoparticles.
- The surface morphology by transmission electron microscopy (TEM).
- Differential scanning calorimetry (DSC) is commonly used techniques to reveal the physicochemical state and possible interactions of the drug and the polymer in nanoparticles

Table: 6.1. Materials and Equipments

Material	Source
Water (distilled)	Prepared in laboratory by distillation
Chitosan low and medium molecular weight	Sigma Aldrich, Bangalore, India
Sodium alginate	National chemical, Mumbai, India
Sodium deoxycholate	Sigma Aldrich, Bangalore, India
Glacial acetic acid, sodium hydroxide, hydrochloric acid	S.D. Fine chemicals, Mumbai, India
Tizanidine HCl	Gift sample from Endoc Pharma, Rajkot, India
Cyclobenzaprine HCl	Gift sample from Ranbaxy, Gurgaon, India
Sodium iodide and Methyl iodide	Spectrochem, Mumbai, India
Thioglycollic acid and Acetonitrile (HPLC grade)	Merck, Mumbai, India
Ellman's reagent	Himedia
Rhodamine B	Himedia
HPLC grade Methanol	Loba Chemicals, India.
Nuclepore Polycarbonate membrane 2 µm 25mm	Whatman, USA
Equipments	**Make**
Calibrated pipettes of 1.0 ml, 5.0 ml and 10.0 ml, volumetric flasks of 10 ml, 25 ml, 50 ml and 100 ml capacity, Funnels (i.d. 5.0 cm), beakers (250 ml) and other requisite glasswares	Schott & Corning (India) Ltd., Mumbai
Analytical balance	AX 120, EL 8300, Shimadzu Corp., Japan
pH meter	Pico^{+} Labindia, Mumbai, India
Cyclomixer, magnetic stirrer	Remi Scientific Equipments, Mumbai
Cooling Centrifuge	3K 30, Sigma Laboratory centrifuge, Osterode, GmBH.
Lyophilizer	DW1, 0-60E, Heto Drywinner, Denmark
UV-Visible Spectrophotometer	Shimadzu UV-1601, Japan
Particle and Zeta size Analyzer	Malvern zeta sizer NanoZS, U.K.
Transmission electron microscopy	Morgagni, Philips, Netherlands
^{1}H-NMR	av300, Bruker, UK
HPLC system	LC 20-AT prominence, Shimadzu Corp., Japan
Stability oven	Shree Kailash Industries, Vadodara
Vacuum Pump F16	Bharat Vacuum pumps, Bangalore
Bath sonicator	INCO, Ambala

6.2. Methods

6.2.1. Particle size and zeta potential: A 2.0 mg sample of NPs was suspended in distilled water, and the particle size and zeta potential were measured using the principle of laser light scattering with zeta sizer (Nano-ZS, Malvern Instruments, UK). The observations are tabulated in Table: 6.2. The particle size and zeta potential are shown in Figure: 6.1 and Figure: 6.2, respectively.

6.2.2. Entrapment efficiency: Drug loaded nanoparticles suspension diluted with 1% (v/v) acetic acid solution and sonicated for 30 minutes, filtrated through 0.22 µm microporous membrane. Total drug loading of NPs fromulations was measured into the filtrate using U.V. spectroscopy. The entrapment efficiency was determined upon separation of nanoparticles from the aqueous suspension containing non-entrapped drug by centrifugation at 18000 rpm 4 °C for 30 minutes. The amount of free drug in the supernatant was measured by U.V spectroscopy (Xiaomei et al., 2008). Drug entrapment efficiency (%EE) in the drug loaded nanoparticles was calculated according to the equations below:

$$\% \text{ EE} = \frac{\text{Total amount of drug loading-free drug in supernant}}{\text{Total amount of drug loading}} \times 100$$

The results are recorded in Table: 6.2 for all nanoparticles

6.2.3. *In-vitro* drug release

In vitro release of drug from nanoparticles was carried out in phosphate buffer (pH 5). For this study, nanoparticles suspension was placed in a dialysis bag and immersed in release medium. The entire system was incubated at 37°C with stirring. At predetermined time intervals, samples were withdrawn from the medium and the same volume of fresh release medium was added and samples were analyzed using HPLC (Qi-zhi et al., 2006).

In-vitro release was also performed using Franz diffusion cell. Franz diffusion cell consists of a hollow glass tube in the centre having diameter of 8 mm. The cell has two compartments: (1) Donor (2) Acceptor. Donor compartment is used for holding the test formulation while the acceptor compartment holds the respective diffusion media. *In vitro* release of drug from nanoparticles was carried out in phosphate buffer (pH 5). For this study, nanoparticles suspension was placed on nasal mucosa holding between the donor compartment and acceptor compartment. The entire system was

incubated at 37°C with stirring. At predetermined time intervals, samples were withdrawn from the medium and the same volume of fresh medium was added and samples were analyzed using HPLC. *In vitro* drug release study is a tool that provides an estimate of the *in vivo* pharmacokinetic and pharmacodynamic performance of the formulation.

Results for *In vitro* release profile of TZ loaded and CBZ loaded chitosan, thiolated chitosan/trimethyl chitosan NPs and solutions of both the drugs are shown in Figure 6.3 & Figure 6.4.

6.2.4. Transmission electron microscopy

Nanoparticles were dispersed in de-ionized water at a concentration of 500µg/ml. To measure the morphology and size distribution of nanoparticles, a drop of sample was placed onto a 300-mesh copper grid coated with carbon. The grid was air-dried overnight to remove surface water. Negative staining was performed using a droplet of 2% w/v phosphotungstic acid for NPs. Transmisssion electron microscopy was performed using Morgagni 268, Philips (Netherlands) transmission electron microscope. The TEM of all nanoparticles formulations are shown in Figure 6.5.

6.2.5. Nasal toxicity studies

Freshly excised sheep nasal mucosa mounted on Franz diffusion cells. One mucosa is treating with phosphate buffer (pH 6.4); the other mucosa with Isopropyl alcohol (IPA) and the remaining with NPs formulations after one hr the mucosa rinsed with phosphate buffer (pH 6.4). Nasal mucosa was fixed in 10% buffered formalin (pH 7.2), routinely processed and embedded in paraffin. Paraffin sections (7 µm) were cut on glass slides and stained with hematoxylin and eosin (HE). Sections were examined under a light microscope, to detect any damage to the mucosa during *in vitro* permeation by a pathologist blinded to the study. The sheep nasal mucosa treating with phosphate buffer (pH 6.4)and isopropyl alcohol as positive and negative control respectively (Majithiya et al., 2006). Figures 6.6 show the histopathological images of nasal mucosa for phosphate buffer (pH 6.4), IPA and drug loaded NPs formulations.

6.2.6. Confocal laser scanning microscopy examination

For confocal laser scanning microscopy examinations, nasal mucosa was rinsed with phosphate buffer (pH 6.4) twice; the freshly excised nasal mucosa was placed in a Petri dish. A few drops of the fluorescent probes (Rhodamine B) loaded NPs dispersions in phosphate buffer (pH 6.4) of each formulations and Rhodamine B

solution in phosphate buffer (pH 6.4) were added to the mucosal surface and incubated for 20 minutes at 37.8 °C. After incubation, the treated mucosa was washed gently with phosphate buffer (pH 6.4) to remove the excess NPs. The sample was then mounted on a glass slide and immediately examine under the confocal microscopy. Fluorescent images were obtain using an upright confocal laser scanning microscope (LSM510, Carl Zeiss, Germany) equipped with 543 nm excitation laser HeNe1 and emission long pass filter 560 nm (LP560) (Law et al., 2001). Figures 6.7 & Figure 6.8 shows the Confocal images of Mucosal surface and after Z sectioning of nasal mucosa for Rhodamine B and Rhodamine B loaded chitosan, thiolated chitosan and trimethyl chitosan NPs.

6.3. Results and Discussions

6.3.1. Particle size and zeta potential:

The particle size and zeta potential for LMC-TZ NPs, LMC-CBZ, MMC-TZ NPs, MMC-CBZ NPs, LMTC-TZ NPs, LMTC-CBZ NPs, MMTC-TZ NPs, MMTC-CBZ NPs, LMTMC-TZ NPs, LMTMC-CBZ NPs, MMTMC-TZ NPs, MMTMC-CBZ NPs are recorded in Table: 6.2. The particle size and zeta potential graphs are shown in Figure: 6.1 and Figure: 6.2, respectively.

Table: 6.2. Characterization of optimized chitosan, thiolated chitosan and trimethyl chitosan NPs

Formulation	Chitosan/Thiolated chitosan/Trimethyl chitosan (mg/ml)	Sodium alginate (mg/ml)	Drug /RB (mg/ml)	Sodium deoxy cholate (mg/ml)	Ratio	Particle size (nm)	Zeta potential (mV)	Entrapment efficiency (%)
LMC-TZ NPs	1 (pH 5)	0.5 (pH 9)	2.5	-	Chitosan solution to sodium alginate solution (2:1)	473.5 ± 13.5	22.8±0.876	44.69±3.5
LMC-CBZ NPs	1 (pH 5)	0.5 (pH 9)	2.5	-	Chitosan solution to sodium alginate solution (2:1)	472.6±12.7	24.7±0.98	62.27±6.1
MMC-TZ NPs	1 (pH 5)	0.5 (pH 9)	2.5	-	Chitosan solution to sodium alginate solution (2:1)	598.7±1.8	23.8 ± 0.987	46.65± 2.4
MMC-CBZ NPs	1 (pH 5)	0.5 (pH 9)	2.5	-	Chitosan solution to sodium alginate solution (2:1)	628.2±13.1	25.1±1.1	64.14±6.4
LMTC-TZ NPs	2	0.5	2	10	Thiolated chitosan :sodium alginate:drug:sodium deoxycholate solution (7:1:1:1)	262.5 ±12.4	12.9±1.44	68.8±6.34
LMTC-CBZ NPs	2	0.5	2	10	Thiolated chitosan :sodium alginate:drug:sodium deoxycholate solution (7:1:1:1)	272.1±11.5	20.9±1.7	70.45±4.3
MMTC-TZ NPs	2	0.5	2	10	Thiolated chitosan :sodium alginate:drug:sodium deoxycholate solution (7:1:1:1)	264.9 ±15	14.5 ± 1.1	72.2± 3.4
MMTC-CBZ NPs	2	0.5	2	10	Thiolated chitosan :sodium alginate:drug:sodium deoxycholate solution (7:1:1:1)	282.9±15.6	27.7±1.2	80.20±3.2
LMTMC-TZ NPs	1	2	2	10	Trimethyl chitosan :sodium alginate:drug:sodium deoxycholate solution (7.9:0.7:0.7:0.7)	168.0±10.2	13.4 ± 1.1	66.90±1.2
LMTMC-CBZ NPs	1	2	2	10	Trimethyl chitosan :sodium alginate:drug:sodium deoxycholate solution (7.9:0.7:0.7:0.7)	184.6±13.9	13.9±1.2	71.75±5.4
MMTMC-TZ NPs	1	2	2	10	Trimethyl chitosan :sodium alginate:drug:sodium deoxycholate solution (7.9:0.7:0.7:0.7)	226.6±18.1	16.7 ± 1.5	62.27±1.8
MMTMC-CBZ NPs	1	2	2	10	Trimethyl chitosan :sodium alginate:drug:sodium deoxycholate solution (7.9:0.7:0.7:0.7)	274.5±21.3	15.9±1.1	72.88±2.1
LMC-RB NPs	1 (pH 5)	0.5 (pH 9)	2.5	-	Chitosan solution to sodium alginate solution (2:1)	463.9 ± 18.1	21.3±0.763	40.34±2.5

MMC-RB NPs	1 (pH 5)	0.5 (pH 9)	2.5	-	Chitosan solution to sodium alginate solution (2:1)	621.8±16.8	24.8±0.988	63.78±4.3
LMTC-RB NPs	2	0.5	2	10	Thiolated chitosan :sodium alginate:RB:sodium deoxycholate solution (7:1:1:1)	262.9±15.9	17.8±2.1	65.89±3.1
MMTC-RB NPs	2	0.5	2	10	Thiolated chitosan :sodium alginate:RB:sodium deoxycholate solution (7:1:1:1)	276.2±13.9	18.3±1.4	75.57±4.1
LMTMC-RB NPs	1	2	2	10	Trimethyl chitosan :sodium alginate:RB:sodium deoxycholate solution (7.9:0.7:0.7:0.7)	176.8±11.7	12.1±1.1	68.23±2.9
MMTMC-RB NPs	1	2	2	10	Trimethyl chitosan :sodium alginate:RB:sodium deoxycholate solution (7.9:0.7:0.7:0.7)	280.1±17.9	16.1±1.9	69.76±3.9

(Mean ± S.D., *n* = 3)

LMC-TZ NPs- Low molecular weight Tizanidine HCl loaded chitosan nanoparticles
LMC-CBZ NPs- Low molecular weight Cyclobenzaprine HCl loaded chitosan nanoparticles
MMC-TZ NPs-Medium molecular weight Tizanidine HCl loaded chitosan nanoparticles
MMC-CBZ NPs-Medium molecular weight Cyclobenzaprine HCl loaded chitosan nanoparticles
LMTC-TZ NPs- Low molecular weight Tizanidine HCl loaded thiolated chitosan nanoparticles
LMTC-CBZ NPs- Low molecular weight Cyclobenzaprine HCl loaded thiolated chitosan nanoparticles
MMTC-TZ NPs- Medium molecular weight Tizanidine HCl loaded thiolated chitosan nanoparticles
MMTC-CBZ NPs- Medium molecular weight Cyclobenzaprine HCl loaded thiolated chitosan nanoparticles
LMTMC-TZ NPs- Low molecular weight Tizanidine HCl loaded trimethyl chitosan nanoparticles
LMTMC-CBZ NPs- Low molecular weight Cyclobenzaprine HCl loaded trimethyl chitosan anoparticles
MMTMC-TZ NPs- Medium molecular weight Tizanidine HCl loaded trimethyl chitosan nanoparticles
MMTMC-CBZ NPs- Medium molecular weight Cyclobenzaprine HCl loaded trimethyl chitosan nanoparticles
LMC-RB NPs- Low molecular weight Rhodamine B loaded chitosan nanoparticles
MMC-RB NPs- Medium molecular weight Rhodamine B loaded chitosan nanoparticles
LMTC-RB NPs- Low molecular weight Rhodamine B loaded thiolated chitosan nanoparticles
MMTC-RB NPs- Medium molecular weight Rhodamine B loaded thiolated chitosan nanoparticles
LMTMC-RB NPs- Low molecular weight Rhodamine B loaded trimethyl chitosan nanoparticles
MMTMC-RB NPs- Medium molecular weight Rhodamine B loaded trimethyl chitosan nanoparticles
SA-Sodium alginate
SDC-Sodium deoxycholate

(a) LMC-TZ NPs

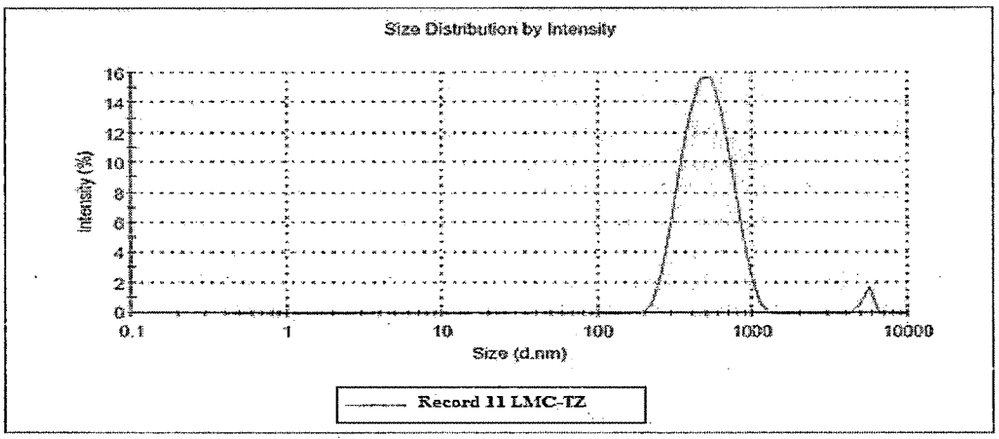

(b) LMC-CBZ NPs

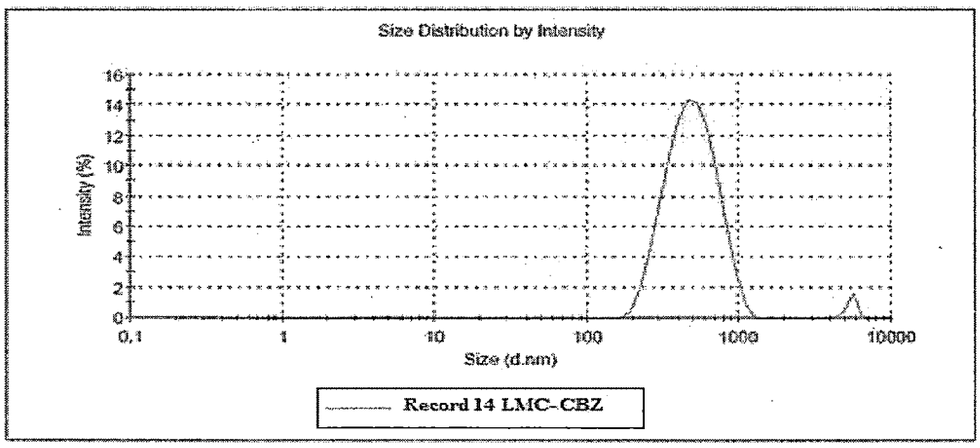

(c) MMC-TZ NPs

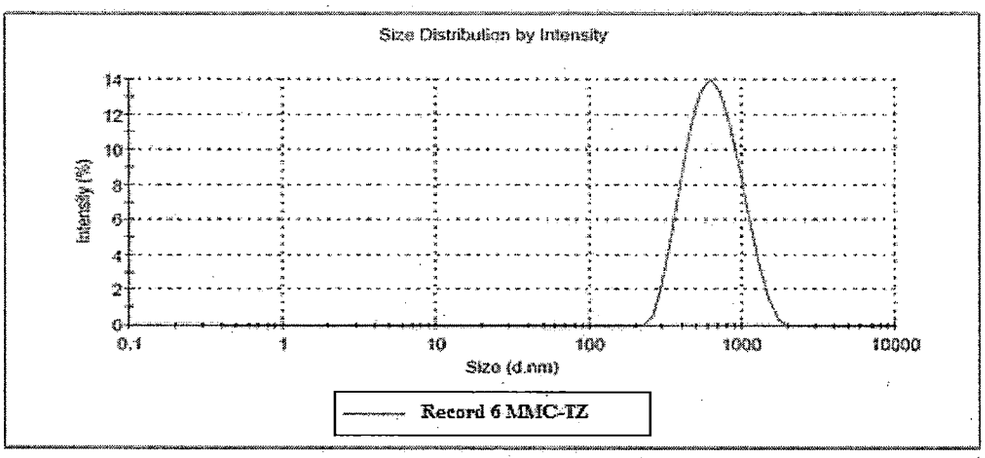

(d) MMC-CBZ NPs

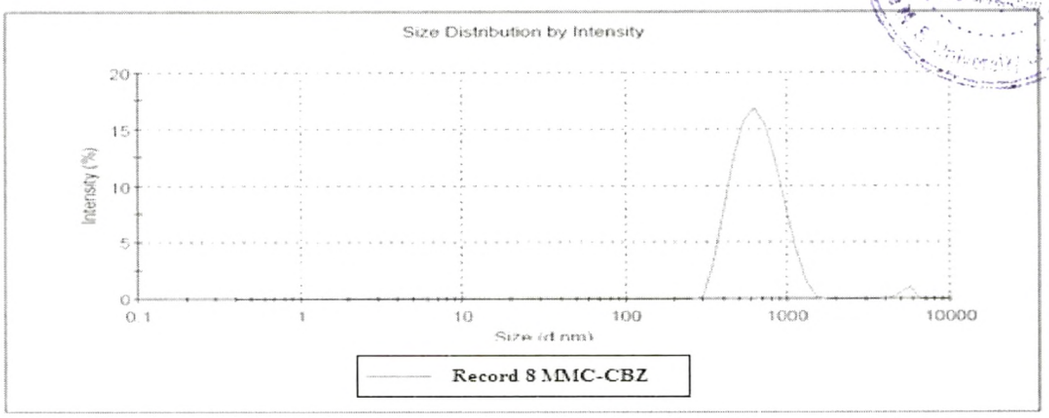

(e) LMTC-TZ NPs

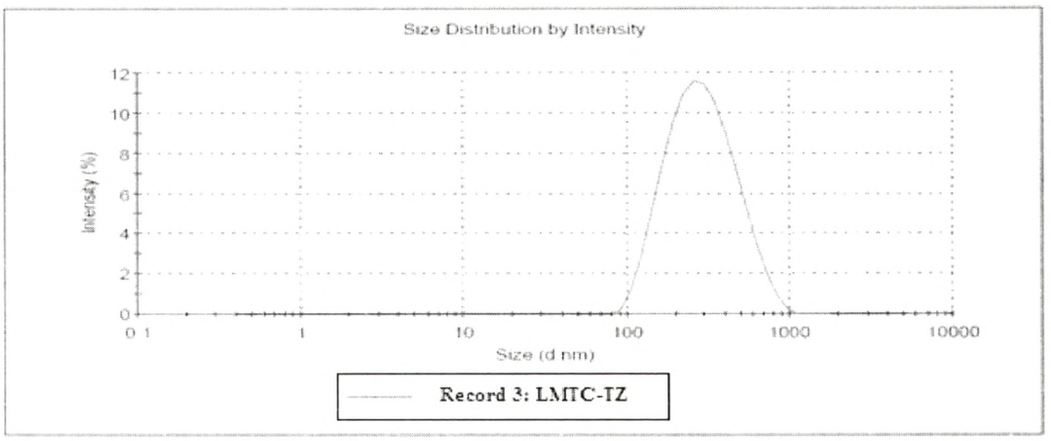

(f) LMTC-CBZ NPs

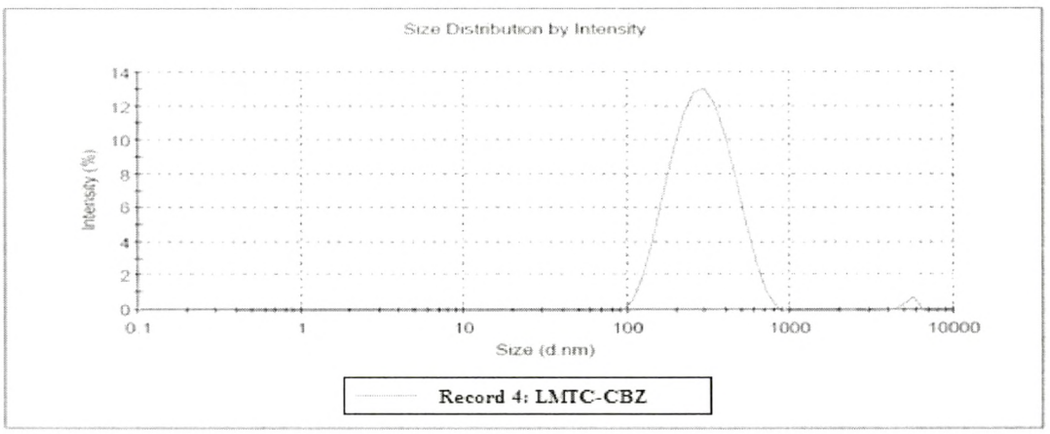

(g) MMTC-TZ NPs

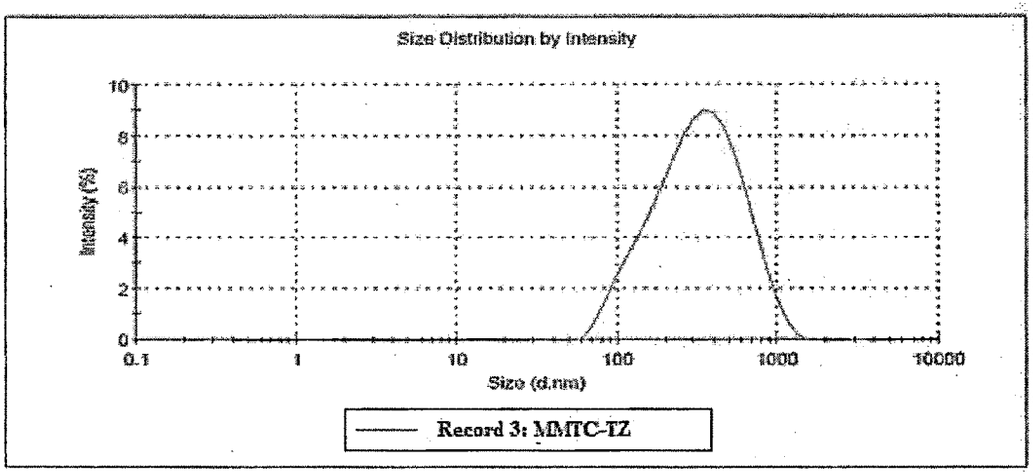

(h) MMTC-CBZ NPs

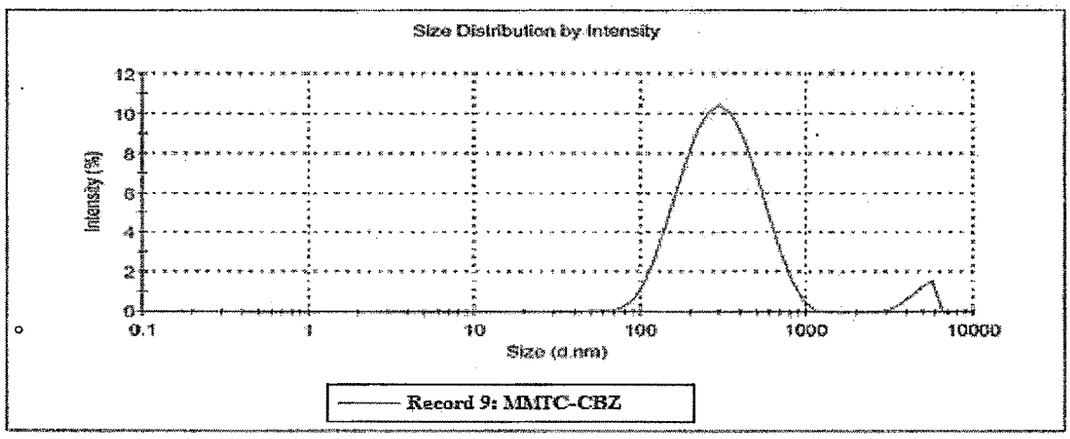

(i) LMTMC-TZ NPs

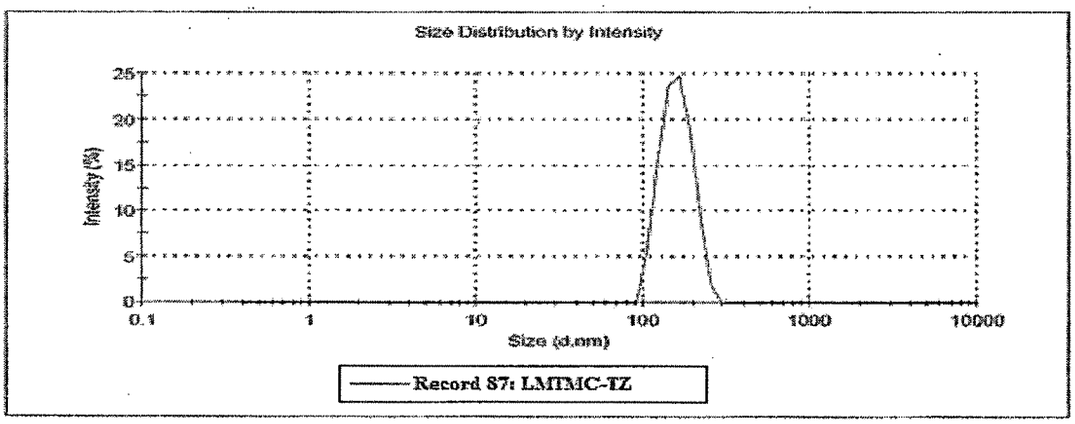

(j) LMTMC-CBZ NPs

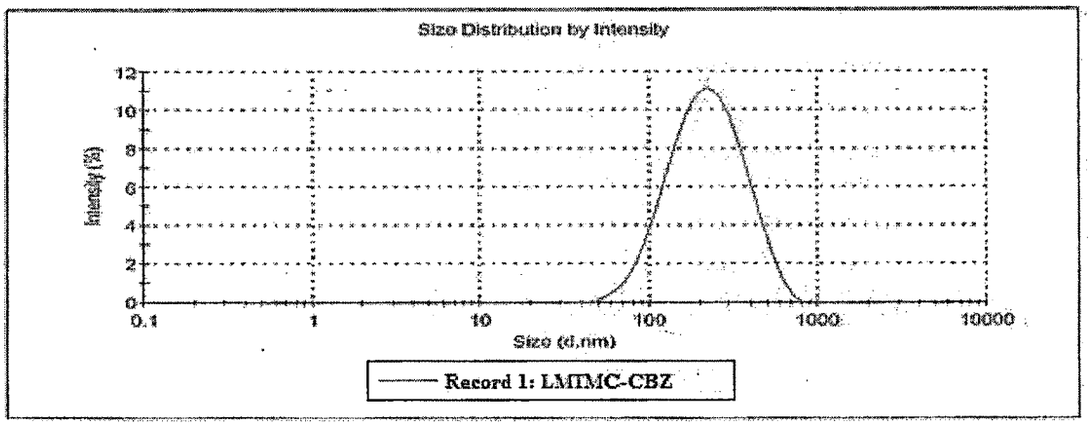

(k) MMTMC-TZ NPs

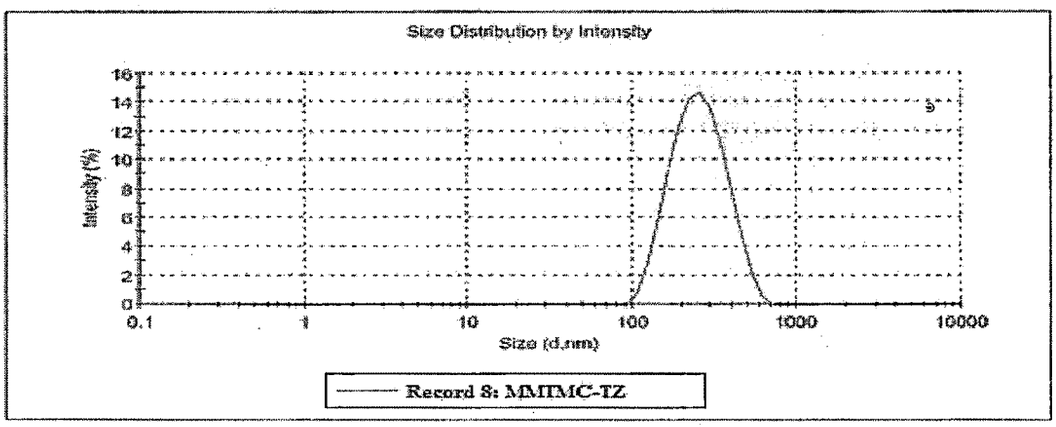

(l) MMTMC-CBZ NPs

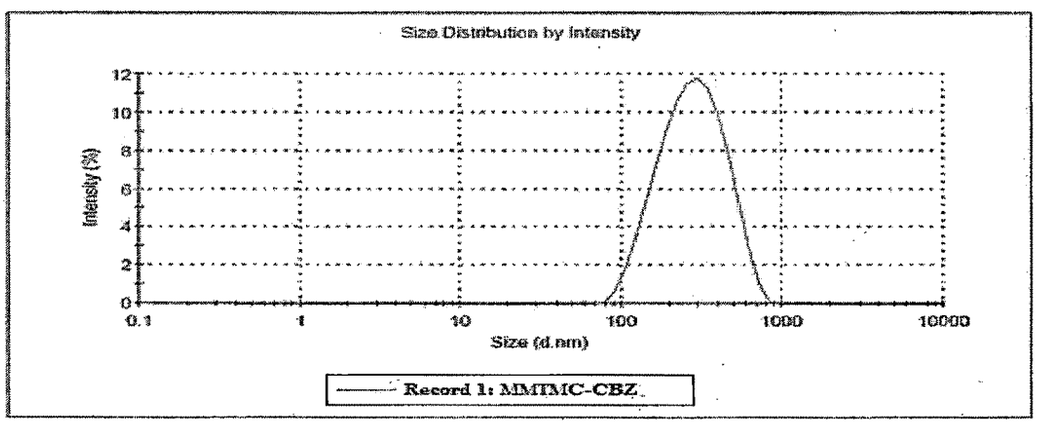

Figure 6.1: Particle size distribution plots of : (a) LMC-TZ NPs (b) LMC-CBZ NPs(c) MMC-TZ NPs (d) MMC-CBZ NPs (e) LMTC-TZ NPs (f) LMTC-CBZ NPs (g) MMTC-TZ NPs (h) MMTC-CBZ NPs (i) LMTMC-TZ NPs (j) LMTMC-CBZ NPs (k) MMTMC-TZ NPs (l) MMTMC-CBZ NPs

(a) LMC-TZ NPs

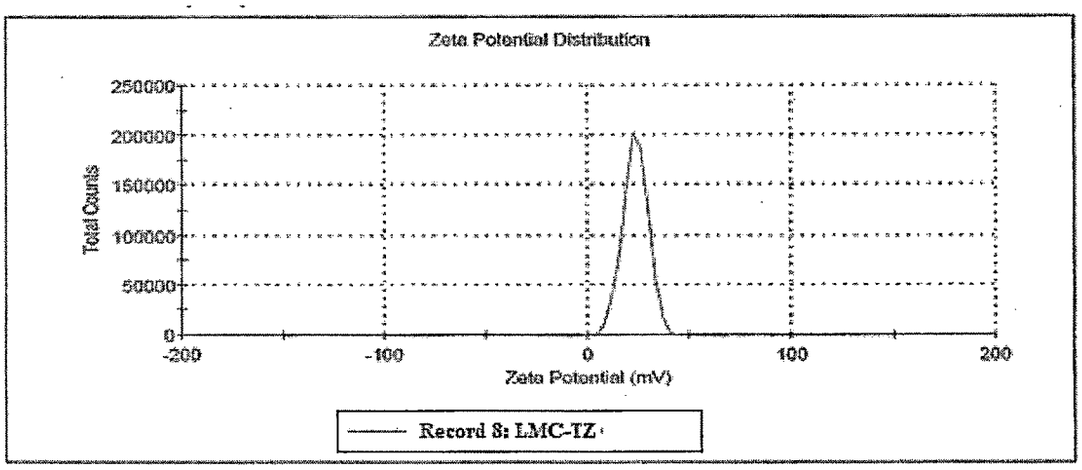

(b) LMC-CBZ NPs

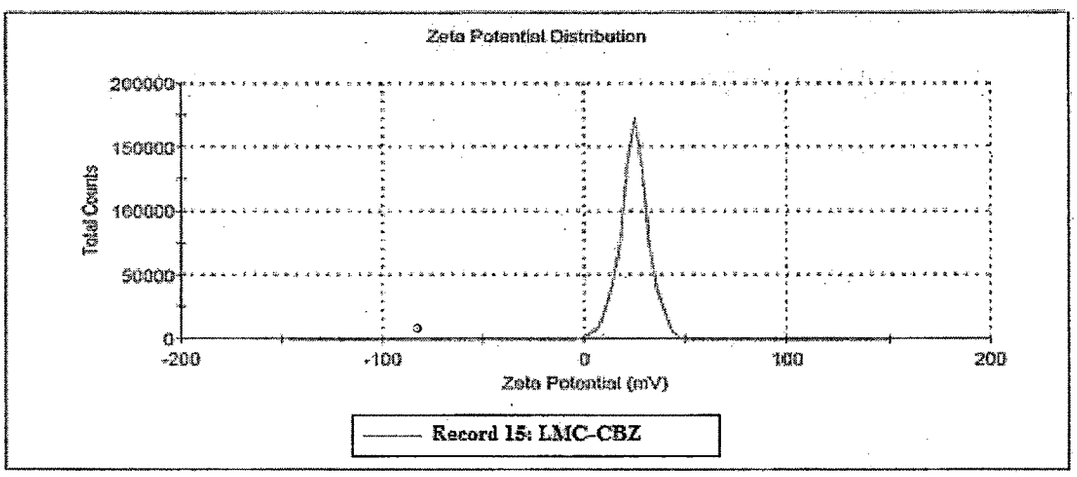

(c) MMC-TZ NPs

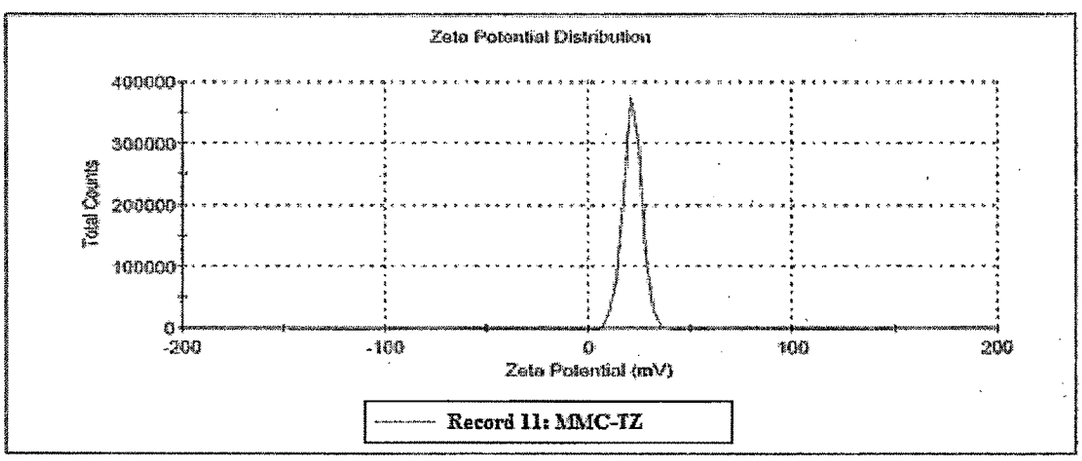

d) MMC-CBZ NPs

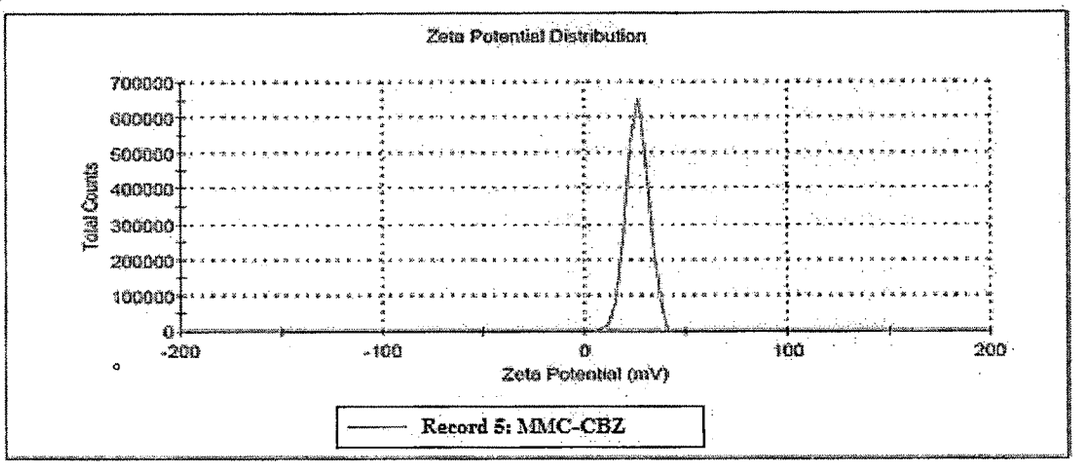

(e) LMTC-TZ NPs

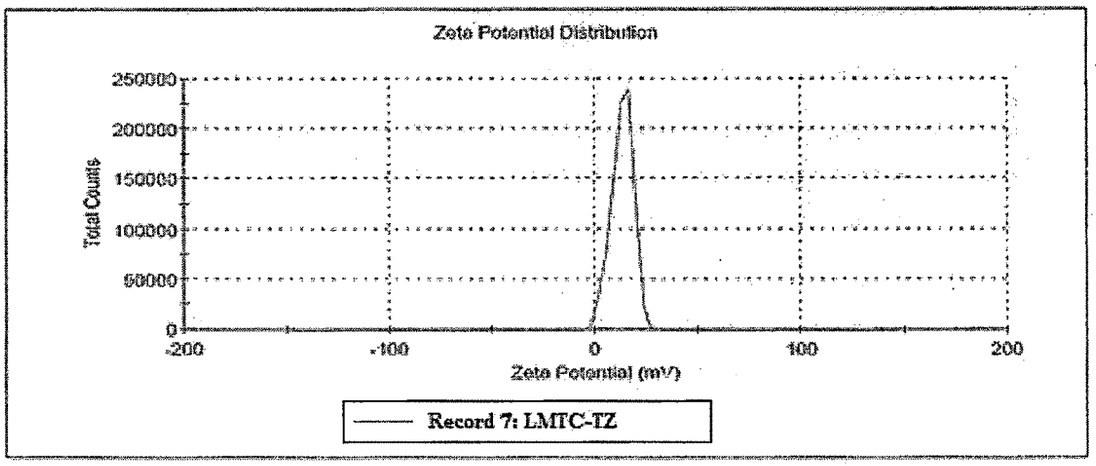

(f) LMTC-CBZ NPs

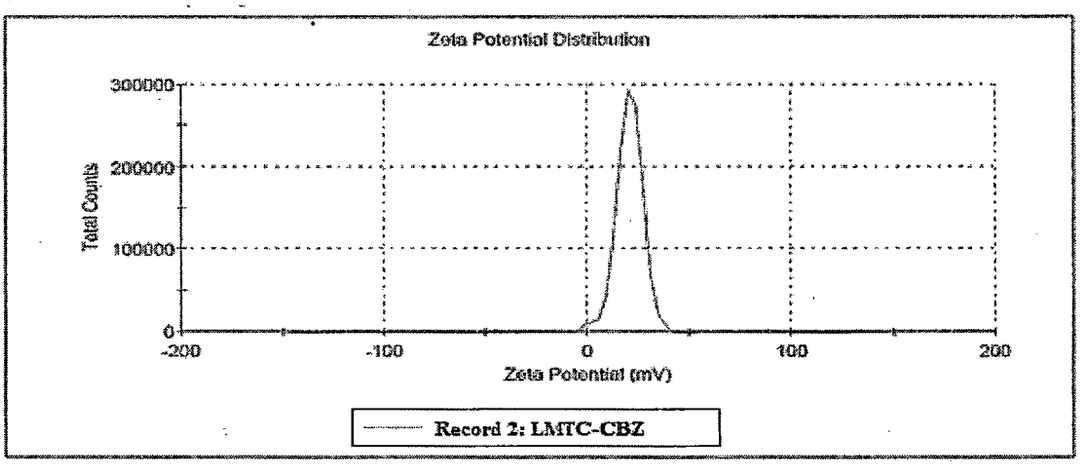

(g) MMTC-TZ NPs

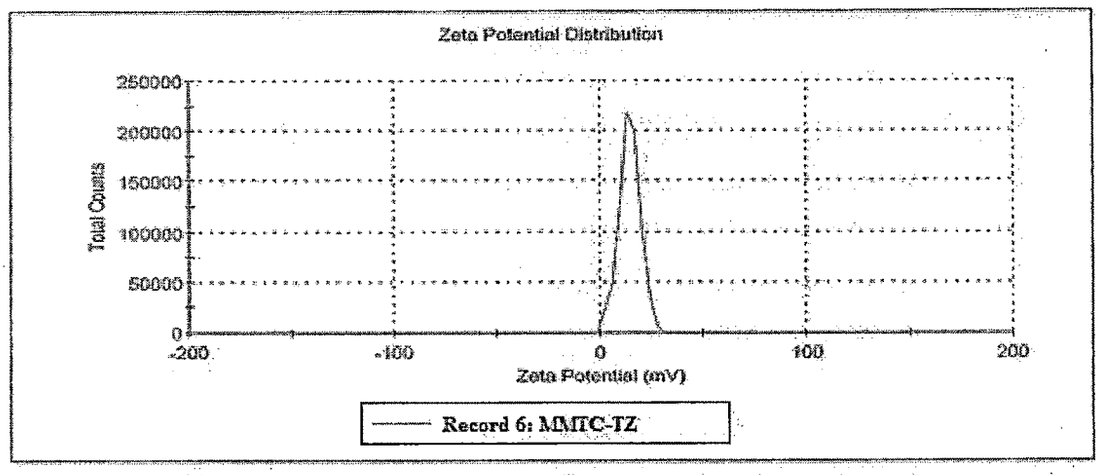

(h) MMTC-CBZ NPs

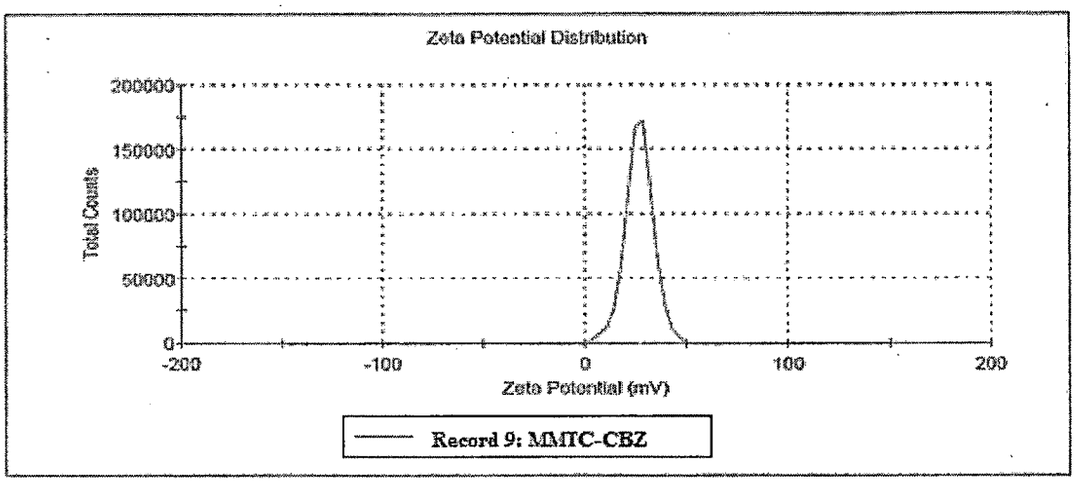

(i) LMTMC-TZ NPs

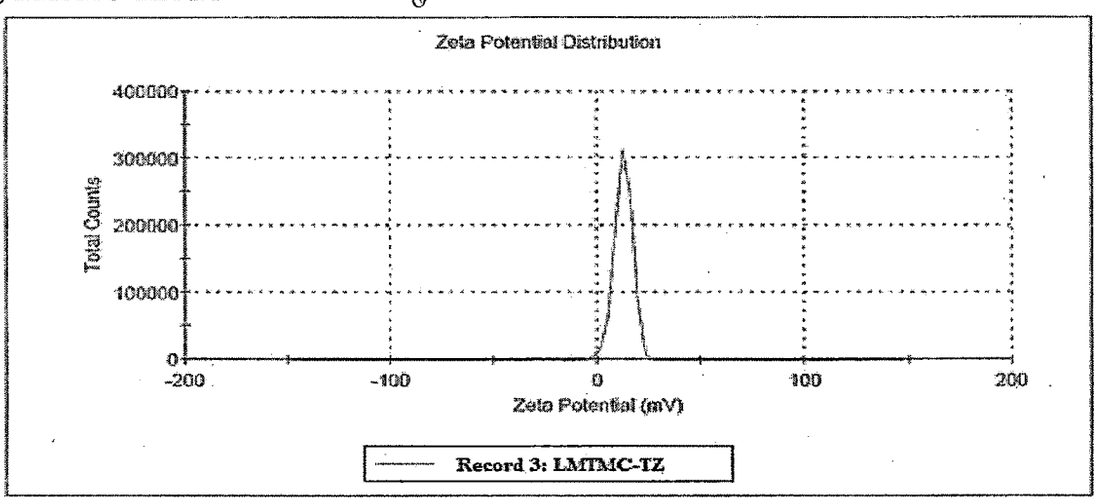

(j) LMTMC-CBZ NPs

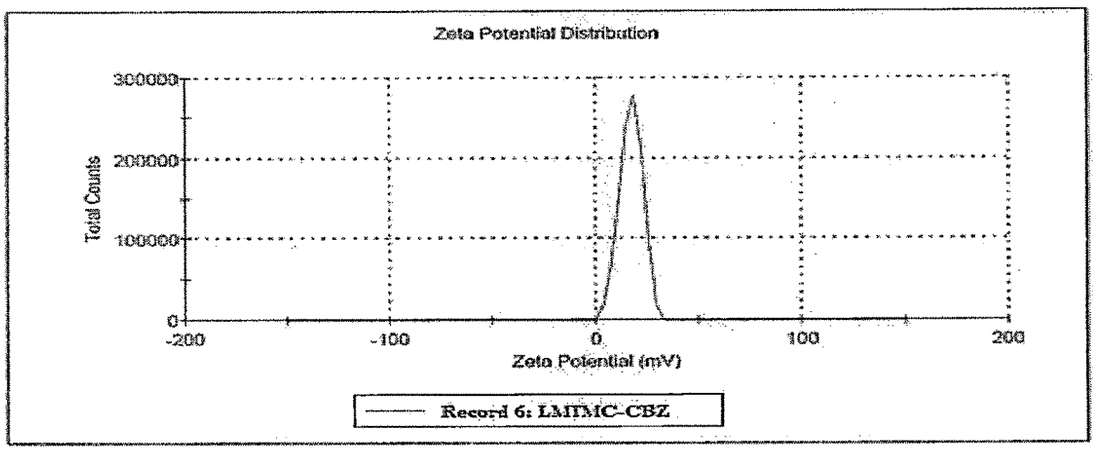

(k) MMTMC-TZ NPs

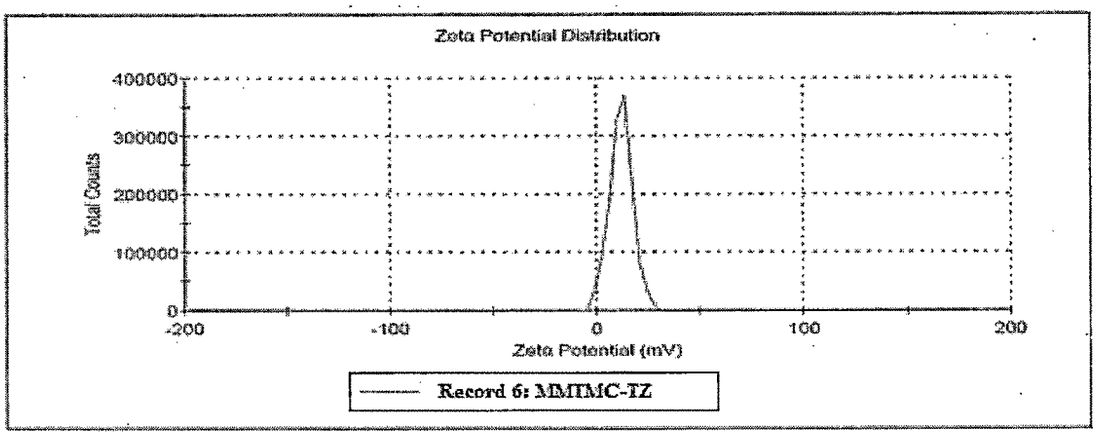

(l) MMTMC-CBZ NPs

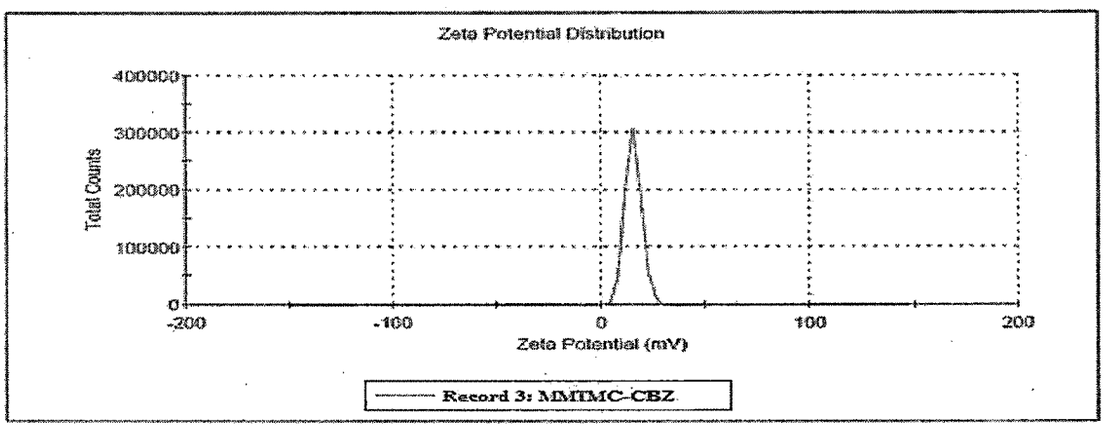

Figure 6.2: Zeta potential plots of : (a) LMC-TZ NPs (b) LMC-CBZ NPs(c) MMC-TZ NPs (d) MMC-CBZ NPs (e) LMTC-TZ NPs (f) LMTC-CBZ NPs (g) MMTC-TZ NPs (h) MMTC-CBZ NPs (i) LMTMC-TZ NPs (j) LMTMC-CBZ NPs (k) MMTMC-TZ NPs (l) MMTMC-CBZ NPs

The particle size of chitosan nanoparticles was found to higher than the particle size of thiolated chitosan and trimethyl chitosan NPs. This result may be due the higher solubility of thiolated chitosan and trimethyl chitosan than the chitosan at physiological pH. The mean hydrodynamic diameter of these types of nanoparticles showed a clear increase with the molecular weight of trimethyl chitosan and thiolated chitosan, which is in agreement with previous works (Chauvierre et al., 2003, Bertholon-Rajot et al., 2005). To elucidate the influence of chitosan, trimethyl chitosan and thiolated chitosan molecular weight on the particle size, as the molecular weight increases the particle size was increased and this trend may be explained by the fact that a medium molecular weight chitosan can more interact and associate drug more efficiently than a lower molecular weight chitosan. The factor is out-weighted by the fact that medium molecular weight chitosan is less soluble compared to low molecular weight chitosan and as a result, an increase in particle diameter or even aggregation may be obtained (Wu et al., 2005). Chitosan free amino groups were responsible for the measured positive zeta potential values obtained for all formulations, which might ensure the electrostatic interactions with the anionic groups of the mucus.

6.3.2. Entrapment efficiency:

Drug entrapment efficiency (%EE) in the drug loaded nanoparticles was calculated according to the equations below:

$$\% \text{ EE} = \frac{\text{Total amount of drug loading-free drug in supernant}}{\text{Total amount of drug loading}} \times 100$$

Drug entrapment was also increased in thiolated chitosan NPs and trimethyl NPs than the chitosan NPs. These results may be due to the use of sodium deoxycholate as a anionic surfactant. Formation of drug-sodium deoxycholate complexes, which can adsorbed more on the positively charged thiolated chitosan and trimethyl chitosan than the highly cationic drug (Carmen et al., 2009). As with increase in the concentration of sodium deoxycholate solution, the size was decreased and surface area was increased. Hence, more drug-sodium deoxycholate complexes adsorbed on the surface of thiolated and trimethyl chitosan leads to high drug entrapment. The results are recorded in Table 6.2 for all nanoparticles.

6.3.3. *In-vitro* drug release

In vitro release of drug from nanoparticles was carried out in phosphate buffer (pH 5) using both dialysis bag (to see the release of drug from the formulation) and nasal

mucosa (to see the diffusion of drug from the biological membrane) (Qi-zhi et al., 2006). Results for *In vitro* release profile of TZ loaded and CBZ loaded chitosan/ thiolated chitosan/trimethyl chitosan NPs and solutions of both the drugs, are shown in Figure 6.3 & Figure 6.4.

(a)

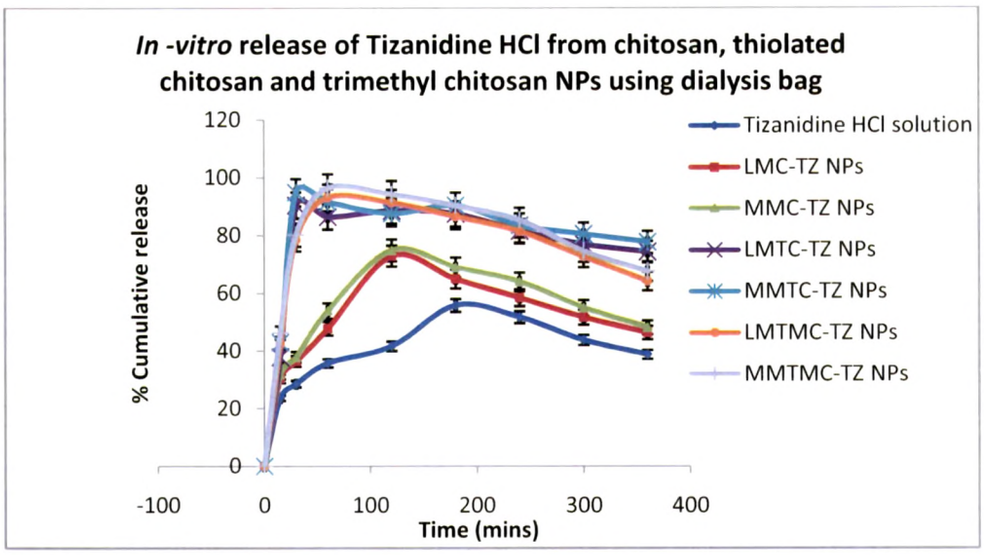

(Mean ± S.D., *n* = 3)

(b)

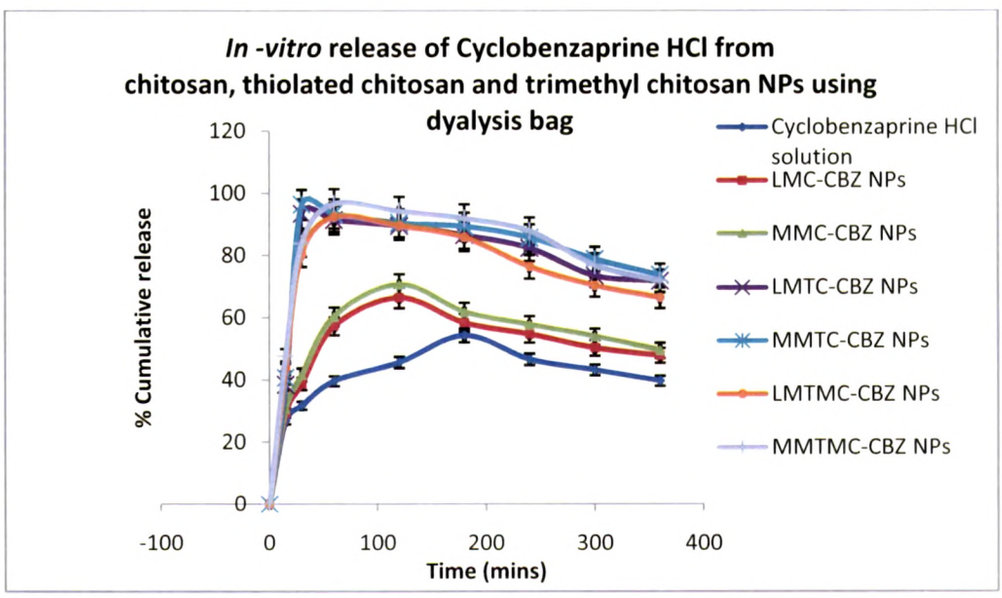

(Mean ± S.D., *n* = 3)

Figure 6.3: (a) *In -vitro* release of tizanidine HCl from chitosan, thiolated chitosan and trimethyl chitosan NPs using dialysis bag (b) *In -vitro* release of cyclobenzaprine HCl from chitosan, thiolated chitosan and trimethyl chitosan NPs using dialysis bag

(a)

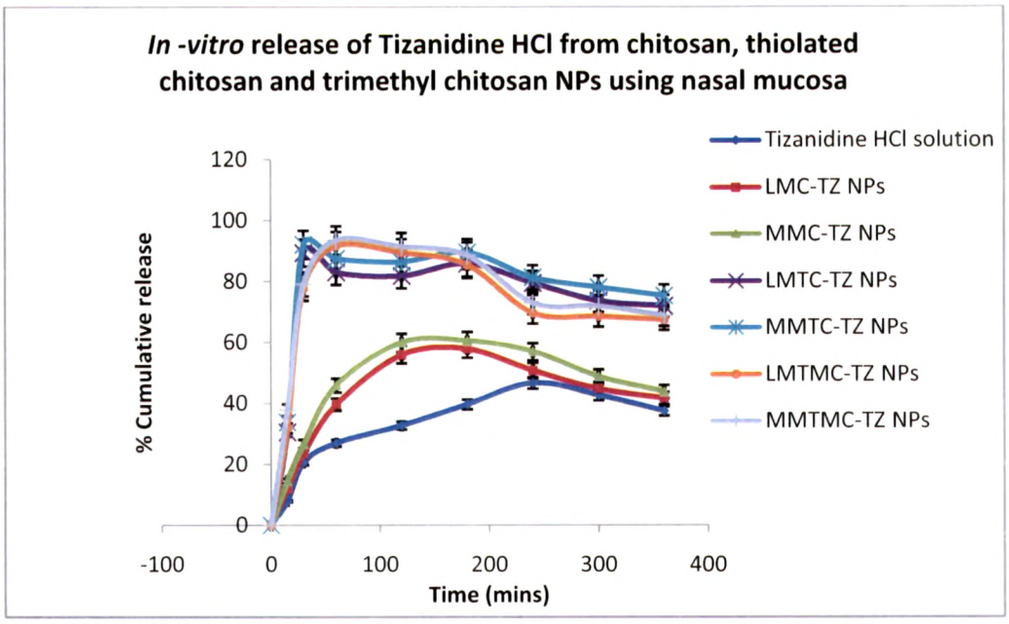

(Mean ± S.D., *n* = 3)

(b)

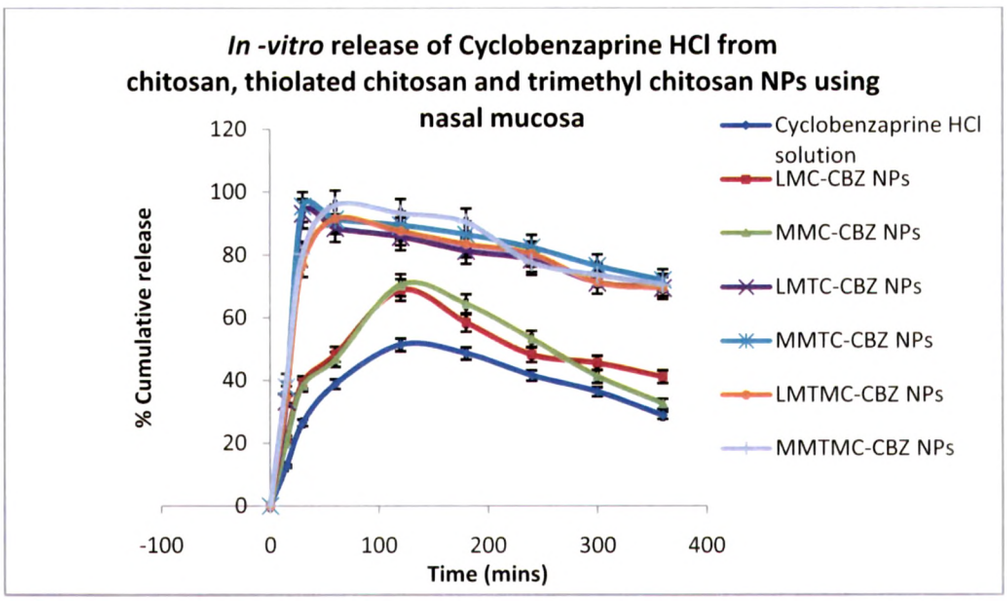

(Mean ± S.D., *n* = 3)

Figure 6.4: (a) *In -vitro* release of tizanidine HCl from chitosan, thiolated chitosan and trimethyl chitosan NPs using nasal mucosa (b) *In -vitro* release of cyclobenzaprine HCl from chitosan, thiolated chitosan and trimethyl chitosan NPs using nasal mucosa

Statistical data analyses were performed using the Student's t test with $p < 0.05$ as the minimal level of significance. All values are expressed as the means ± S.D.

The maximum 51 to 55 % of drug release was found in 2-3 hrs for TZ and CBZ solution. TZ loaded and CBZ loaded chitosan NPs shows higher drug release around 65-72 % in 2-3 hrs than the drug solution. Tizanidine HCl loaded and Cyclobenzaprine HCl loaded thiolated chitosan NPs and trimethyl chitosan NPs shows the comparative faster and higher release around 88-96 % in 60 minutes. The significant change in results may be due to the improved solubility of thiolated chitosan and trimethyl chitosan at physiological pH than the chitosan. Thiolated chitosan and trimethyl chitosan were found to have high mucoadhesive strength and high solubility than the chitosan so the more drug was absorbed and permeate faster through on the nasal mucosa.

6.3.4. Transmission electron microscopy

The TEM images of LMC-TZ NPs, LMC-CBZ NPs, MMC-TZ NPs, MMC-CBZ NPs, LMTC-TZ NPs, LMTC-CBZ NPs, MMTC-TZ NPs, MMTC-CBZ NPs, LMTMC-TZ NPs, LMTMC-CBZ NPs, MMTMC-TZ NPs, MMTMC-CBZ NPs are shown in Figure 6.5. TEM images of NPs showed uniform particle size in nanometer range.

(a) LMC-TZ NPs (b) LMC-CBZ NPs

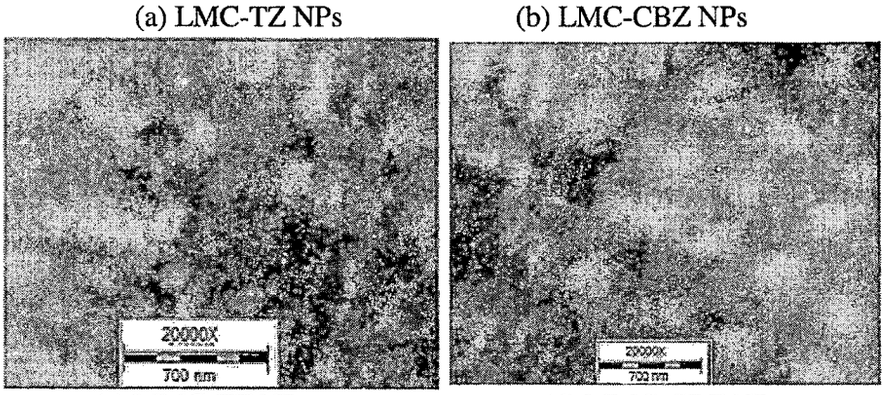

(c) MMC-TZ NPs (d) MMC-CBZ NPs

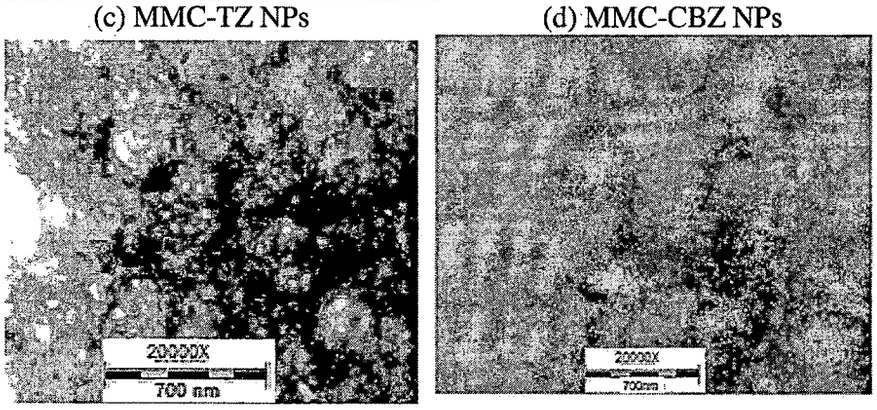

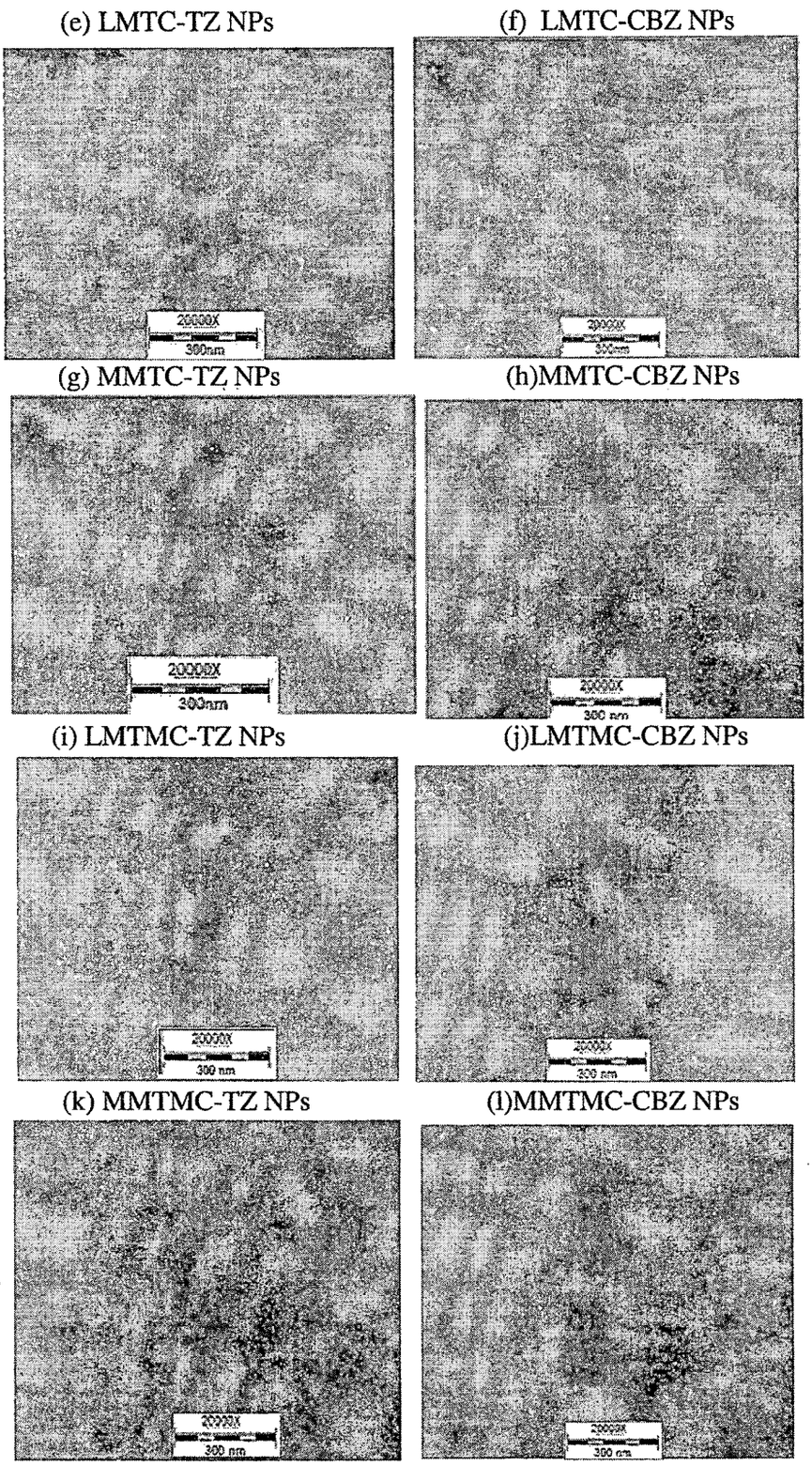

Figure 6.5: TEM image of : (a) LMC-TZ NPs (b) LMC-CBZ NPs(c) MMC-TZ NPs (d) MMC-CBZ NPs (e) LMTC-TZ NPs (f) LMTC-CBZ NPs (g) MMTC-TZ NPs (h) MMTC-CBZ NPs (i) LMTMC-TZ NPs (j) LMTMC-CBZ NPs (k) MMTMC-TZ NPs (l) MMTMC-CBZ NPs

6.3.5. Nasal toxicity studies

Freshly excised sheep nasal mucosa mounted on Franz diffusion cells. One mucosa is treating with phosphate buffer (pH 6.4); the other mucosa with Isopropyl alcohol (IPA) and the remaining with NPs formulations after one hr the mucosa rinsed with phosphate buffer (pH 6.4). Nasal mucosa was fixed in 10% buffered formalin (pH 7.2), routinely processed and embedded in paraffin. Paraffin sections (7 µm) were cut on glass slides and stained with hematoxylin and eosin (HE). Sections were examined under a light microscope, to detect any damage to the mucosa during *in vitro* permeation by a pathologist blinded to the study. The sheep nasal mucosa treating with phosphate buffer (pH 6.4) and isopropyl alcohol as positive and negative control respectively (Majithiya et al., 2006). Figures 6.6 show the histopathological images of nasal mucosa for phosphate buffer (pH 6.4). IPA and all drug loaded NPs formulations.

(a) LMC-TZ NPs

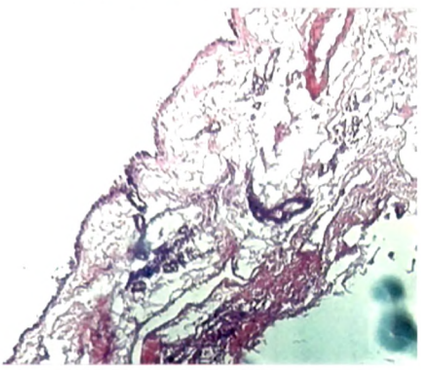

(b) LMC-CBZ NPs

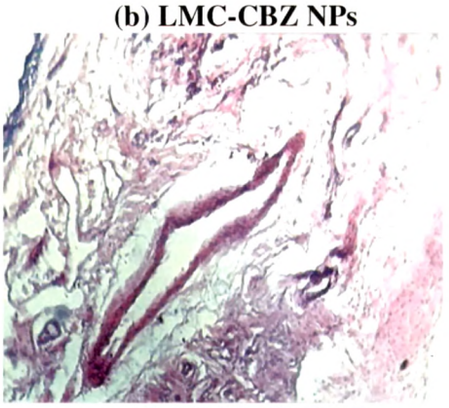

(c)MMC-TZ NPs

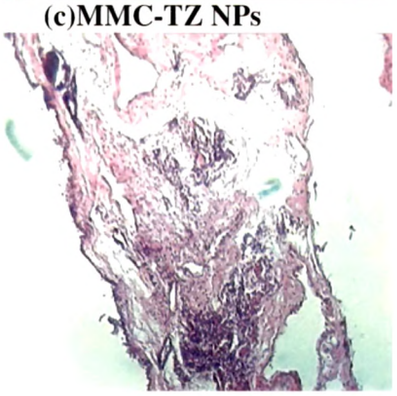

(d) MMC-CBZ NPs

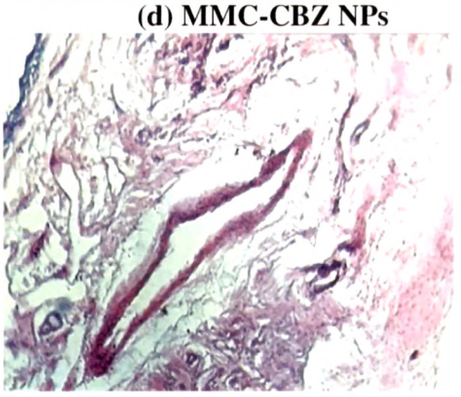

(e) LMTC-TZ NPs

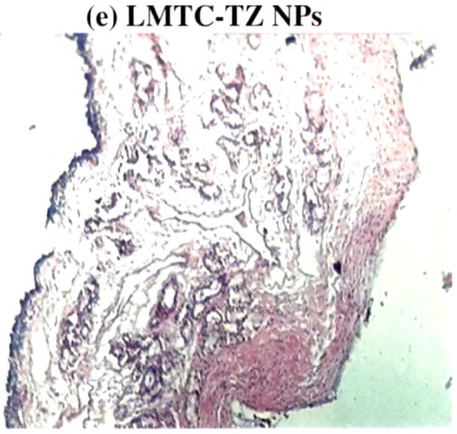

(f) LMTC-CBZ NPs

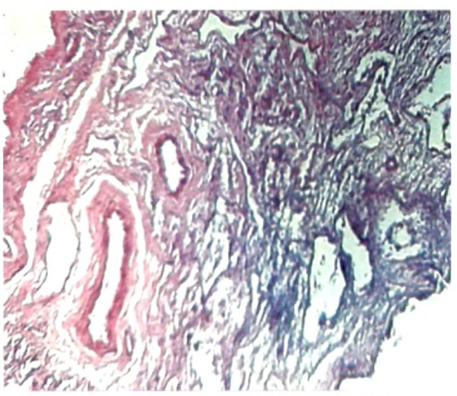

(g)MMTC-TZ NPs

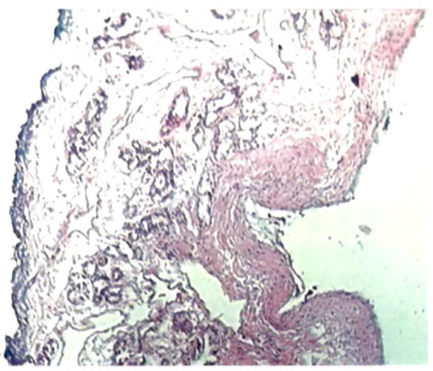

(h) MMTC-CBZ NPs

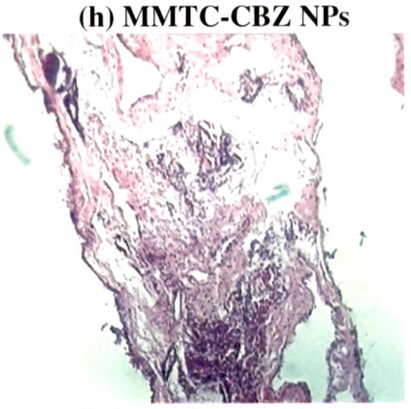

(i) LMTMC-TZ NPs

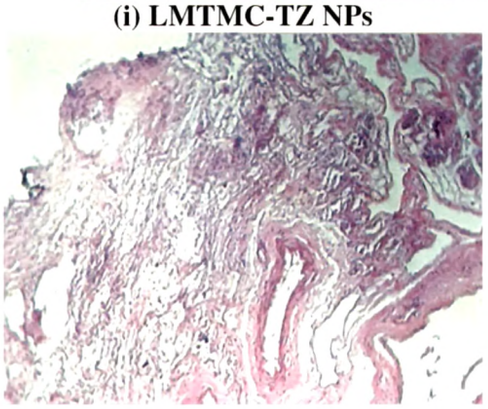

(j) LMTMC-CBZ NPs

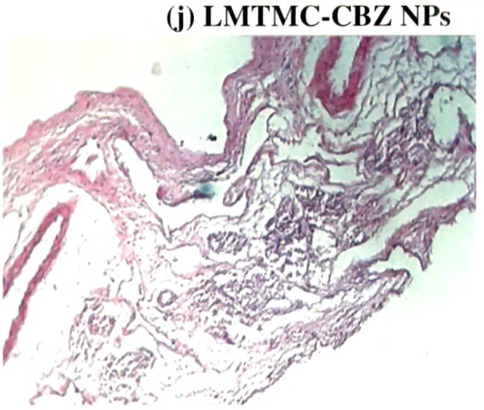

(k) MMTMC-TZ NPs

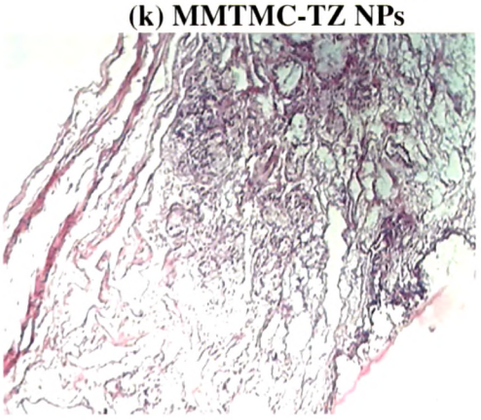

(l) MMTMC-CBZ NPs

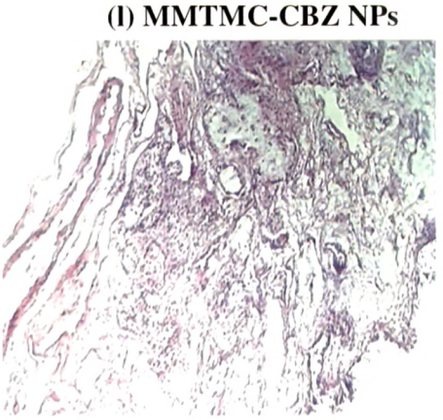

(m) Phosphate buffer (pH 6.4) **(n) Isopropyl alcohol**

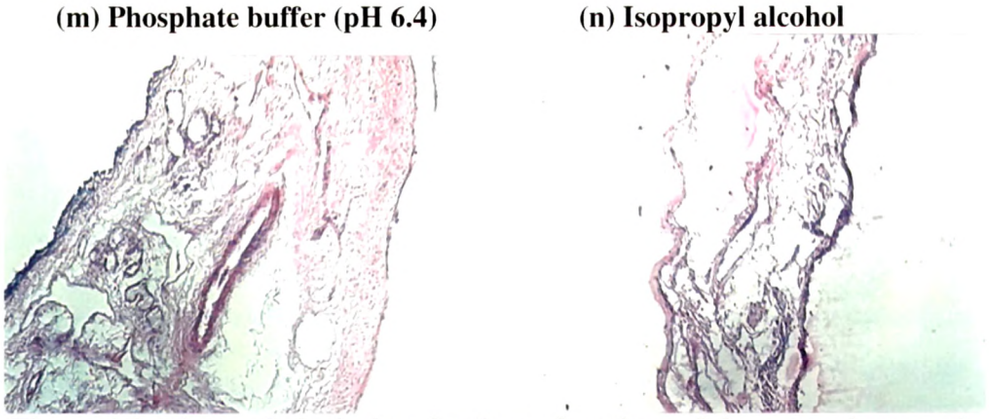

Figure 6.6: Histopathological evaluations of sections of sheep nasal mucosal membrane: a) LMC-TZ NPs (b) LMC-CBZ NPs(c) MMC-TZ NPs (d) MMC-CBZ NPs (e) LMTC-TZ NPs (f) LMTC-CBZ NPs (g) MMTC-TZ NPs (h) MMTC-CBZ NPs (i) LMTMC-TZ NPs (j) LMTMC-CBZ NPs (k) MMTMC-TZ NPs (l) MMTMC-CBZ NPs (m) Phosphate buffer (pH 6.4) (n) IPA

The microscopic observations indicate that the optimized formulations have no significant effect on the microscopic structure of mucosa. As shown in Figure 6.6 neither cell necrosis nor removal of the epithelium from the nasal mucosa was observed after permeation of NPs formulations. The epithelium layer was intact and there were no alterations in basal membrane and superficial part of submucosa as compared with phosphate buffer (pH 6.4) treated mucosa. Thus, the develop formulations seem to be safe with respect to nasal administration

6.3.6. Confocal laser scanning microscopy examination

Figures 6.7 & Figure 6.18 shows the confocal images of mucosal surface and after Z sectioning of nasal mucosa for Rhodamine B (RB) solution, Rhodamine B loaded chitosan/ thiolated chitosan/trimethyl chitosan NPs.

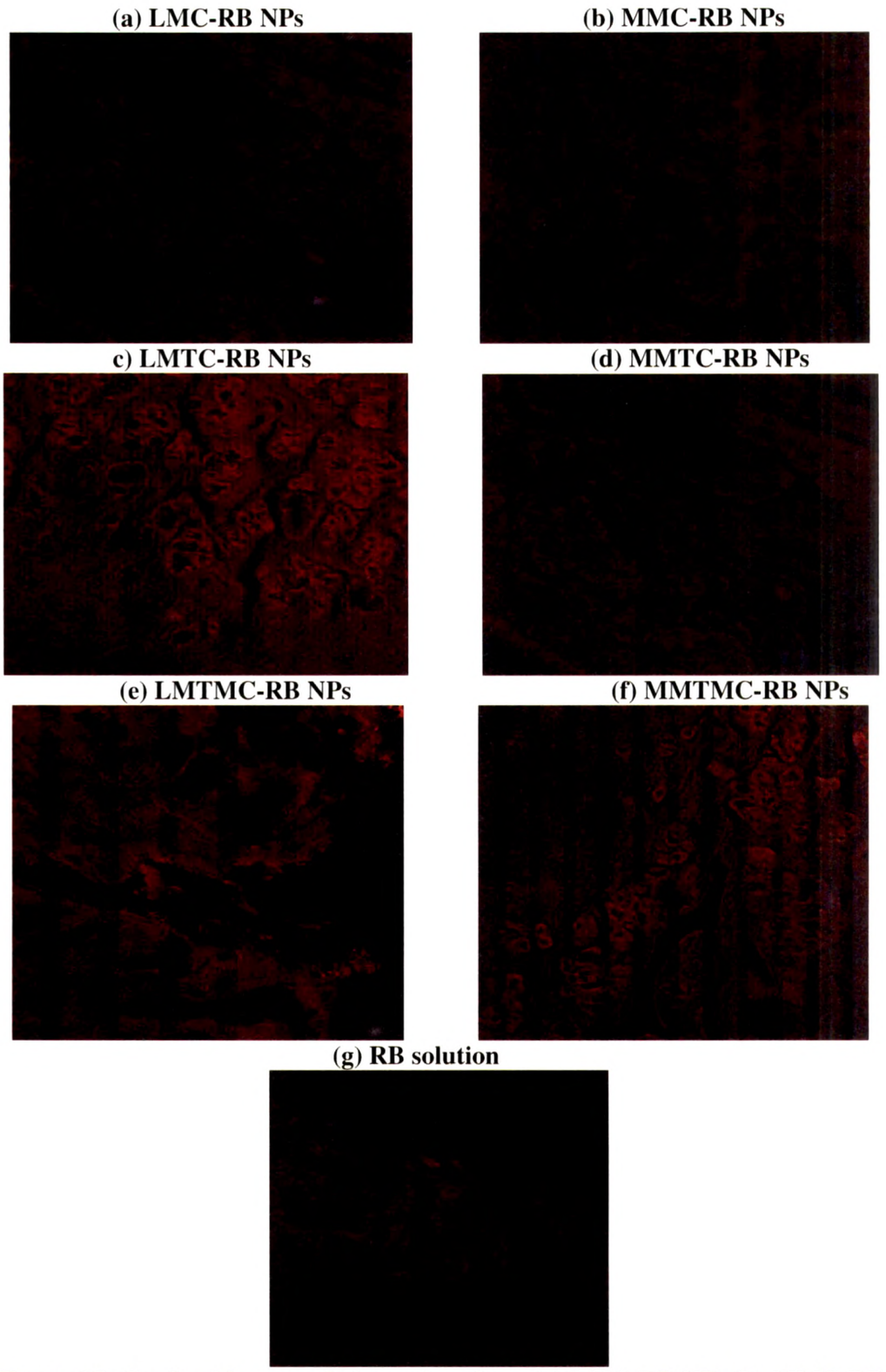

Figure 6.7: Confocal images of Mucosal surface: (a) LMC-RB NPs (b) MMC-RB NPs(c) LMTC-RB NPs (d) MMTC-RB NPs (e) LMTMC-RB NPs (f) MMTMC-RB NPs (g)RB solution

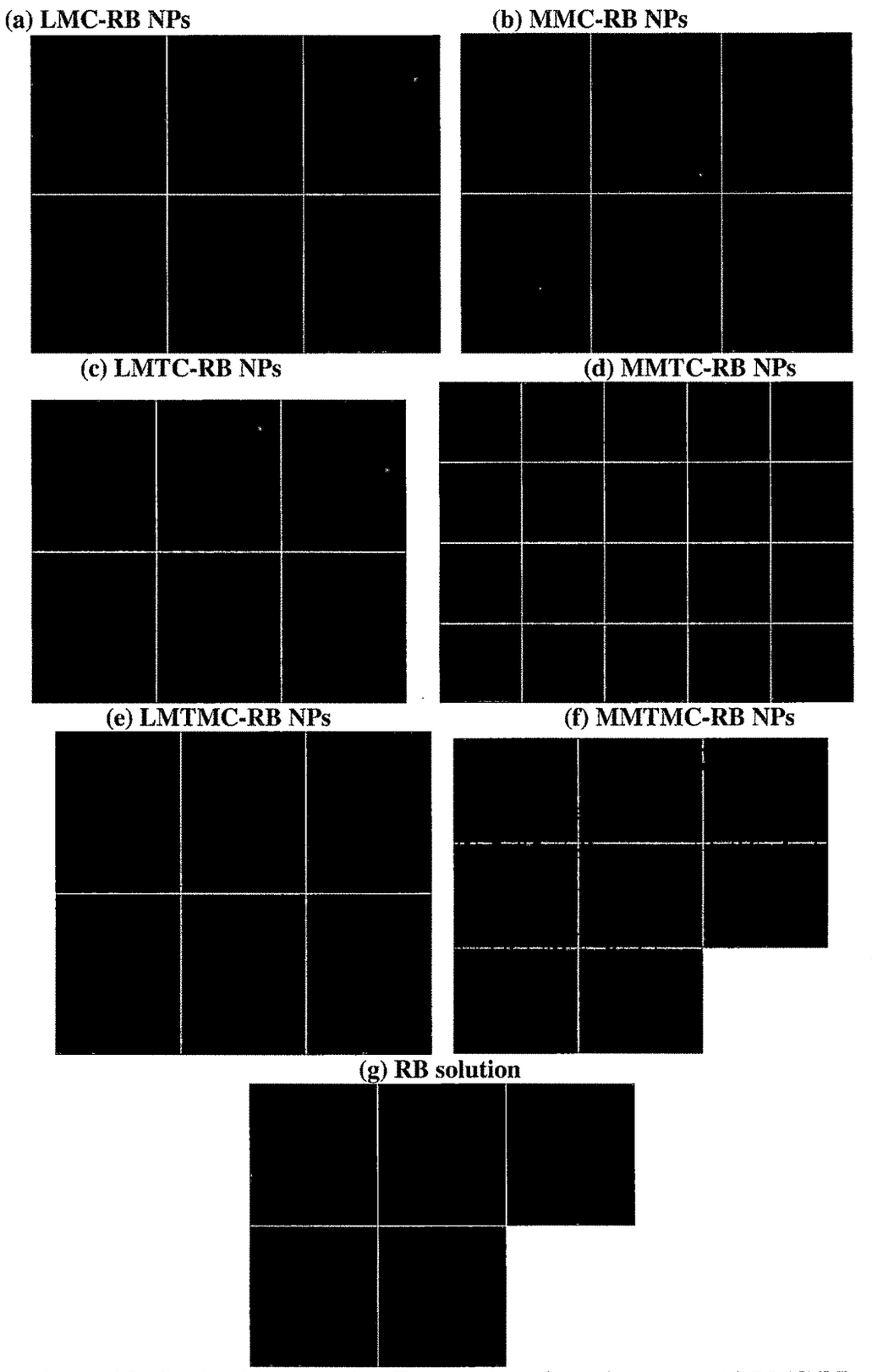

Figure 6.8: Confocal images after Z sectioning of nasal mucosa: (a) LMC-RB NPs (b) MMC-RB NPs(c) LMTC-RB NPs (d) MMTC-RB NPs (e) LMTMC-RB NPs (f) MMTMC-RB NPs (g) RB solution

As observed by confocal laser scanning examination, the positively charged chitosan thiolated chitosan and trimethyl chitosan NPs performed stronger interaction with the nasal mucosa than the Rhodamine B solution. This bioadhesive effect resulted in an enhanced contact time of the thiolated chitosan NPs and trimethyl chitosan NPs on the negatively charged nasal mucosa than the chitosan NPs and Rhodamine B solution. The findings may be explained by the formation of covalent bonds between the thiol groups of thiolated chitosan and cysteine residue by the formation of ionic bond between positive charges of TMC and negatively charged sialic groups on the mucus protein structure. This effect leads to high concentration of drug on the penetration site to promote an effective penetration of drug through the nasal mucosa. Images after the Z sectioning of nasal mucosa showed that the higher penetration of thiolated NPs and trimethyl NPs than the chitosan NPs and rhodamine B.

6.4. Conclusions

After characterizations of all formulations, we may concluded that the TZ loaded and CBZ loaded chitosan, thiolated chitosan and trimethyl chitosan NPs have small particle size (<700nm), positive zeta potential with higher mucoadhesive strength and drug permeation through nasal mucosa that suitable for intranasal administration. *In vitro* release studies shows that the comparatively high and fast release of TZ and CBZ from the thiolated chitosan and trimethyl chitosan NPs than the chitosan NPs and drug solution. The smooth and spherical surface of NPs was confirmed using TEM. The epithelium layer was intact and there were no alterations in basal membrane and superficial part of submucosa as compared with phosphate buffer (pH 6.4) treated mucosa. Thus, the develop formulations seem to be safe with respect to nasal administration. Both the drug loaded chitosan/thiolated chitosan/trimethyl chitosan NPs were further subjected to stability studies according to ICH guidelines (Chapter 7).

6.5. References

Carmen, P., Hayat, O. (2009). Biodegradable Nanoparticles Incorporating Highly Hydrophilic Positively Charged Drugs. United State patent, 424489.

Law, S.L., Huang, K.J., Chou, H.Y. (2001). Preparation of desmopressin-containing liposomes for intranasal delivery. Journal of Controlled Release, 70(3), 375–382.

Majithiya, R.J., Ghosh, P.K., Umrethia, M.L., Murthy, R.S.R. (2006). Thermoreversible-mucoadhesive Gel for Nasal Delivery of Sumatriptan. AAPS PharmSciTech.,7(3), E1-7.

Qi-zhi, Z., Liu-Sheng, Z., Yan, Z., Wen-Ming, J., Wei, L., Zhen-Qi, S., Xin-Guo, J., Shou-Kuan, F. (2006). The brain targeting efficiency following nasally applied MPEG-PLA nanoparticles in rats. Journal of Drug Targeting, 14(5), 281–290.

Wang, X., Chi, N., Xing, T. (2008). Preparation of estradiol chitosan nanoparticles for improving nasal absorption and brain targeting. European Journal of Pharmaceutics and Biopharmaceutics. 70(3), 735–740.

Wu, Y., Yang, W., Wang, C., Hu, J., Fu, S. (2005). Chitosan nanoparticles as a novel delivery system for ammonium glycyrrhizinate, International Journal of pharmaceutics. 295 (1-2) 235–245.